

This is an Open Access document downloaded from ORCA, Cardiff University's institutional repository: <https://orca.cardiff.ac.uk/id/eprint/160549/>

This is the author's version of a work that was submitted to / accepted for publication.

Citation for final published version:

Hills, Rachel, Mossman, Jim A., Bratt-Leal, Andres M., Tran, Ha, Williams, Roy M., Stouffer, David G., Sokolova, Irina V., Sanna, Pietro P., Loring, Jeanne F. and Lelos, Mariah J. 2023. Neurite outgrowth and gene expression profile correlate with efficacy of human induced pluripotent stem cell-derived dopamine neuron grafts. *Stem Cells and Development* 32 (13-14) , pp. 387-397. 10.1089/scd.2023.0043

Publishers page: <http://dx.doi.org/10.1089/scd.2023.0043>

Please note:

Changes made as a result of publishing processes such as copy-editing, formatting and page numbers may not be reflected in this version. For the definitive version of this publication, please refer to the published source. You are advised to consult the publisher's version if you wish to cite this paper.

This version is being made available in accordance with publisher policies. See <http://orca.cf.ac.uk/policies.html> for usage policies. Copyright and moral rights for publications made available in ORCA are retained by the copyright holders.



Neurite outgrowth and gene expression profile correlate with efficacy of human induced pluripotent stem cell-derived dopamine neuron grafts

Running Head: Correlates of efficacy of grafted human DA neurons

Rachel Hills¹, Jim A. Mossman², Andres M. Bratt-Leal^{3,4‡}, Ha Tran^{3,4‡}, Roy M. Williams^{3‡}, David G. Stouffer³, Irina V. Sokolova⁵, Pietro P. Sanna⁵, Jeanne F. Loring^{3*}, Mariah J. Lelos^{1*}

¹Brain Repair Group, School of Biosciences, Museum Avenue, Cardiff University, Cardiff, CF10 3AX, U.K.

²Independent bioinformatics consultant, Del Mar, CA 92014

³Department of Molecular Medicine, Center for Regenerative Medicine, Scripps Research, 10550 North Torrey Pines Road, La Jolla, CA, 92037, USA.

⁴Summit For Stem Cell Foundation, San Diego, California, USA

⁵Department of Immunology and Microbiology, Scripps Research, 10550 North Torrey Pines Road, La Jolla, CA, 92037, USA

‡Currently affiliation: Aspen Neuroscience, San Diego, CA 92121

*Corresponding authors

Corresponding author contacts: lelosmj@cardiff.ac.uk, jloring@scripps.edu

Abstract

Transplantation of human induced pluripotent stem cell-derived dopaminergic (iPSC-DA) neurons is a promising therapeutic strategy for Parkinson's disease (PD). To assess optimal cell characteristics and reproducibility, we evaluated the efficacy of iPSC-DA neuron precursors from two individuals with sporadic PD by transplantation into a hemiparkinsonian rat model after differentiation for either 18 (d18) or 25 days (d25). We found similar graft size and DA neuron content in both groups, but only the d18 cells resulted in recovery of motor impairments. In contrast, we report that d25 grafts survived equally as well and produced grafts rich in tyrosine hydroxylase-positive neurons, but were incapable of alleviating any motor deficits. We identified the mechanism of action as the extent of neurite outgrowth into the host brain, with d18 grafts supporting significantly more neurite outgrowth than non-functional d25 grafts. RNAseq analysis of the cell preparation suggests that graft efficacy may be enhanced by repression of differentiation-associated genes by REST, defining the optimal pre-differentiation state for transplantation. This study demonstrates for the first time that DA neuron grafts can survive well in vivo while completely lacking the capacity to induce recovery from motor dysfunction. In contrast to other recent studies, we demonstrate that neurite outgrowth is the key factor determining graft efficacy and our gene expression profiling revealed characteristics of the cells that may predict their efficacy. These data have implication for the generation of DA neuron grafts for clinical application.

Key Words (10): Cell therapy; neural transplantation; graft; Parkinson's disease; dopamine; neurite outgrowth; hiPSC; behavior; gene expression; rodent model

Introduction

Therapeutic interventions alleviating motor symptoms in Parkinson's disease (PD) typically target replacement of lost dopamine (DA) transmission within the basal ganglia in order to overcome the impact of nigrostriatal degeneration[1]. Cell replacement therapies seek to restore the DA neurons that have lost connections of to medium spiny neurons in the striatum. Clinical trials using fetal tissue containing DA neuron precursor cells as a reparative strategy for PD have demonstrated long-term recovery of function in some patients[2] and graft survival for over 20 years[3].

Human pluripotent stem cells (hPSCs: human embryonic stem cells or human induced pluripotent stem cells) can be differentiated into ventral midbrain DA (vmDA) cells, and these cell therapy products have been widely reported to survive, integrate, release DA and alleviate functional impairments when transplanted into rodent models of PD[4–7]. Cell therapies for PD are moving into an exciting era, with several first-in-human clinical trials using hPSC-derived DA neuron precursors recently begun, or due to commence[8–11].

Most current strategies for cell replacement have relied on a single immunologically unmatched hPSC line to generate DA neuron precursors for transplantation. Since these allogenic approaches require immunosuppression and its associated risks, we are investigating the feasibility of autologous DA neuron replacement. In this study we used induced pluripotent stem cells (iPSCs) from two individuals with idiopathic PD. The primary aims were to assess the reproducibility of the generation of transplant-ready DA neuron precursors, and to identify the point during differentiation for optimal integration and efficacy of the iPSC-DA grafts. We chose 18 days (d18) and 25 days (d25) of differentiation *in vitro*, and phenotyped cultures at the two stages with transcriptome profiling. DA precursors from both donors were transplanted into a hemiparkinsonian rat model. Our data show that regardless of cell line or differentiation stage, all transplanted preparations survived and matured into grafts rich in DA neurons. However, we found that there was a striking difference in efficacy between d18 and d25-differentiated cells from both iPSC lines. The d18 precursors from both lines consistently alleviated motor impairments in the

rat model as measured six months after transplantation, while the d25 cells consistently failed to reverse motor symptoms in this model. Immunohistochemical analysis of the iPSC-DA grafts showed that classic measures of graft volume or DA neuron content did not distinguish efficacious from non-efficacious transplants. Instead, significant differences in the extent of neurite outgrowth from the grafts correlated with the ability to elicit behavioral recovery.

Transcriptome analysis of cell culture phenotype revealed differences between efficacious and non-efficacious DA precursors in expression of genes related to neurite outgrowth, development and plasticity. Interestingly, the efficacious pre-transplantation stage was characterized in both cell lines by the transcriptional repression of a group of neural differentiation-associated genes regulated by REST (RE1 Silencing Transcription Factor); these genes were expressed at the later, non-efficacious stage, accompanied by a decrease in REST expression. This suggests that the optimal cell population would be at a plastic stage that enables response to the host environment by extending neurites and integrating into the brain.

Methods

The results of this study show, in two different patient-derived iPSC lines, that specific characteristics of the cultured cells determine their ability to reverse motor deficits in a rat model of PD, which is dependent on their ability to extend neurites into the host brain. Two iPSC lines (410, 411) were generated from fibroblasts harvested from two people with idiopathic PD (**Figure 1**). The iPSC lines were differentiated *in vitro* to DA neuron precursors for 18 or 25 days to investigate the optimal stage for transplantation. To confirm that the precursors were capable of differentiation into mature DA neurons, both cell lines were differentiated further *in vitro* into mature DA neurons. The precursors harvested after 18 days (410-d18; 411-d18) or 25 days (410-d25; 411-d25) of differentiation were used for transplantation into a rodent model of PD. At the same stages, replicate cultures were analyzed by mRNA sequencing to examine their phenotypic characteristics.

Both cell lines were transplanted into the 6-OHDA lesioned hemiparkinsonian model of PD, at both stages of the differentiation protocol. Other groups of rats remained as naïve controls or lesioned controls. Rats underwent behavioral testing pre- and post-transplantation and brains were taken for histological analysis at 24 weeks post-graft. Histological analysis of the grafts included markers of human cells (HuNu) and mature DA neurons (TH, GIRK2, AADC), as well as two methods of measuring the extent of neurite outgrowth from the TH+ neurons. All experiments were conducted in compliance with the UK Animals (Scientific Procedures) Act 1986 under Home Office Licence No. 30 / 3036 and with the approval of the local Cardiff University Ethics Review Committee. See **Supplemental Methods** for further details.

Results

Both iPSC lines differentiated into mature dopamine neurons in vitro.

To assess the abilities of the two iPSC lines to differentiate into mature dopamine neurons, we cultured them under differentiation conditions for 12 weeks *in vitro*. Both donor-derived iPSC lines differentiated into mature dopamine neurons, showing mature DA neuron markers by immunocytochemistry, bursting activity and mature membrane potential by patch clamp electrophysiology, and HPLC to detect evoked dopamine release (**Figure 2A**).

Behavioral analysis revealed motor recovery after transplantation of earlier (d18) but not later (d25) DA neuron precursors

Multiple behavioral analyses showed that the hemiparkinsonian rats transplanted with the earlier (d18) stage precursors showed reversal of deficits, while those transplanted with the later (d25) stage precursors did not recover. On the amphetamine-induced rotation test, motor recovery was evident after transplantation of earlier (d18) but not later (d25) DA neuron precursors (**Figure 3A,B**; $F_{30,270}=5.59$, $p<0.001$). For the apomorphine-induced rotation test, rats grafted with cells from the earlier stage of differentiation (410-d18 and 411-d18) did not differ from unlesioned control rats, indicating that improvement in the rotational bias was conferred by both cell lines differentiated to d18 (**Supplemental Figure**

1A; $F_{5,50}=6.34$, $p<0.001$). On the gait analysis test, rats grafted with cells from the earlier differentiation stage showed increased stride length relative to lesioned controls, suggesting improvement in gait performance (**Supplemental Figure 4B**; $F_{5,50}=3.27$, $p<0.05$).

Differences in graft size or composition did not explain the difference in efficacy between d18 and d25 precursor grafts.

Immunohistological analysis was used to quantify the number of engrafted human cells (HuNu+), and cells positive for mature DA neuronal markers (TH+, AADC+, GIRK2+) that were detected in both d18 and d25 grafts (**Figure 3C-N**). The analysis showed that none of these characteristics explained the difference in behavioral recovery between the d18 and d25 grafts (**Figure 3F**).

The immunohistochemical analysis revealed variations dependent on cell line and/or stage (days *in vitro*); however, these characteristics could not explain the difference in functional efficacy between the d18 and d25 grafts. In general, d18 grafts were larger (**Figure 3C,D**) and had more cells labeled for TH (**Figure 3F,G**), GIRK2 (**Figure 3I**) and AADC (**Figure 3L**) [minimum $F_{1,11}=6.02$, $p<0.05$]. The density of TH+ neurons (**Figure 3E**) and the percentage of GIRK2+ neurons (**Figure 3J**) was also greater in d18 grafts [minimum $F_{1,11}= 6.32$, $p<0.05$]. But comparison of similar sized grafts makes clear that none of those factors was critical to the behavioral outcome. This is illustrated by comparing a group of grafts of similar size but with different behavioral outcomes. Day 25 (410-d25) and day 18 (411-d18) grafts had different behavioral outcomes, but the non-efficacious day 25 grafts were slightly larger (**Figure 3C,D**), had comparable TH+ density (**Figure 3E**), and contained more TH+ (**Figure 3F**), GIRK2+ (**Figure 3I**) and AADC+ neurons (**Figure 3L**) than the day 18 grafts [minimum $F_{1,11}= 6.97$, $p<0.05$]. In summary, behavioral recovery did not correlate with the number of HuNu+ cells, graft volume, total number of TH+ cells, AADC+ cells, GIRK2+ cells, nor density of TH+ cells (**Figure 4F**). Representative immunohistochemistry for TH+, GIRK2+, AADC+ and HuNu+ neurons is shown in **Figure 3H, K and N**. **Figure 2B** shows representative examples of TH immunolabelling for multiple d18 and d25 grafts at 24 weeks post-transplant.

Functional improvements correlated with significantly more extensive neurite outgrowth from grafts of earlier (d18) cultures than later cultures (d25)

Both manual and automated estimates of graft-derived TH+ fibers revealed significantly more neurite outgrowth and innervation from d18 grafts into the host brain than from d25 grafts (**Figure 4A,G,H; Supplemental Figure 1C,D**; minimum $F_{1,11}=14.31$, $p<0.01$). Even when innervation data were normalized to graft size or TH+ neurons, more innervation was evident in d18 grafts, suggesting that differences in graft integration are due to underlying features of the transplanted cells and are irrespective of graft size or TH+ cell number (**Supplemental Fig 1D**). Moreover, functional recovery on the amphetamine-induced rotation test correlated with all measures of neurite outgrowth (**Figure 4F, Supplemental Figure 1E-J**). Representative images of neurite outgrowth are depicted in **Figure 4B-E**.

Gene expression analysis identified stage-associated signatures of developing DA neuron precursors.

mRNA sequencing was used to compare phenotypic profiles of the cell cultures as they progressed through development toward DA neurons. Principal component analysis (PCA) of the time course of differentiation (d0, d13, d18, d25) showed no overlap among the time points; PC1 separated the undifferentiated iPSC lines from the others and PC2 resolved the later timepoints in a consistent rank order (**Figure 5A**). When only the three differentiation phases (d13, 18, 25), were compared, PC1 separated the three stages of differentiation for both cell lines, and PC2 distinguished the two cell lines that had similar but not identical profiles (**Figure 5B**). The factor loading of the top- and bottom- ranked genes on these PC axes are listed in **Supplemental Table 1A**. Differential expression (DE) analysis comparing the two stages used in the animal studies (d18 and d25) showed 949 genes that were significantly ($FDR<0.05$) differentially expressed. Of these, 520 genes ($FDR<0.05$) were up-regulated in d25 compared to d18 and 429 genes ($FDR<0.05$) were down-regulated (**Figure 6A; Supplemental Table 1B**: genes with negative \log_2 fold change have higher expression at d25 relative to d18). The key processes active in d13, d18 and d25 cultures are listed in **Figure 6B**. Gene Ontology (GO) analysis indicated that the main gene set that was up-regulated at d18 relative to d25 was largely associated with

proliferation. On d25, the up-regulated genes had an overwhelming signal of synapse-related ontologies (**Supplemental Table 1C**).

Transcription binding site motifs for the transcription factors *E2F4*, *FOXM1*, *SIN3A* and *NFYA* (**Figure 5C; Supplemental Table 1D**) were enriched in the genes expressed at higher levels in day 18 cultures compared to the later stage (d25), which is consistent with a pre-differentiated state. Among the genes up-regulated at the later stage (d25) relative to d18, there was a strong enrichment for transcription factor binding site motifs for *REST*, *SUZ12*, *EZH2* and *SMAD4* (**Supplemental Table 1D**). Additionally, as *REST* levels decreased between d18 and d25, expression of neuron-associated genes with REST motifs increased (**Figure 5D-F**).

Discussion

Success of regenerative therapies using pluripotent stem cell-derived cell types is dependent on the demonstration of their functional efficacy, and the maturation stage and plasticity of the cultures is key to achieving this. The efficacy[13] and size[14] of hPSC-derived DA neuron precursor grafts has been linked to the length of time that the cells were differentiated before transplant. We took this concept a step further, using two different iPSC lines derived from people with PD at two time points during *in vitro* differentiation of DA neurons, and found that for both cell lines, the critical factor determining efficacy of the transplants was not size nor composition of the grafts, but the extent of neurite outgrowth into the host striatum. Both cell lines at both time points, 18 or 25 days of differentiation, engrafted well. The grafts were variable in volume, density and quantity of iPSC-derived dopaminergic neurons, but these characteristics did not correlate with the functional efficacy. Only the cells from the earlier time point were efficacious, and differed from the later time point's ineffective grafts in only one characteristic: the ability to react to the host brain by producing extensive neurite growth.

These results suggest that the efficacious cells were in a poised state, activated to extend neurites when they encountered target cells in the striatum, while the ineffective cells, while able to survive, had decreased ability to form functional connections with the host brain. To investigate this idea, we analyzed the cells *in vitro* by gene expression profiling.

Gene expression profiling predicts the differentiation abilities of pluripotent stem cells[15,16] and it is likely to prove useful for prediction of other qualities, such as post-transplantation characteristics. Our results are consistent with the idea that the cultures that were functionally effective were poised to begin to mature, but had not quite initiated the processes leading to functional neurons. One gene that is of particular interest is *REST* (RE1 silencing transcription factor), which codes for a transcription factor that acts as a repressor of genes involved in neural maturation; its expression is thought to allow a pool of neural precursors to accumulate during processes of neural differentiation in embryogenesis[16]. In our cultures, *REST* decreased considerably at d25; in addition, at d25, genes with *REST* transcription factor binding motifs were upregulated, which is consistent with removal of REST-mediated repression. *REST* expression and expression of the regulated genes could prove to be useful markers to assess an optimal stage of transplantation of future cell therapy products.

Some genes that were specifically upregulated in d18 cells are associated with neurite outgrowth, including LIN28A, FLRT3, and ITGA5. LIN28A ($\log_2FC=3.8$) codes for a post-transcriptional regulator of miRNAs associated with embryogenesis and has been linked to axonal regeneration [17–20]. Overexpression of LIN28A in DA neurons has been reported to increase dendrite length, graft volume, and TH+ content, and enhance functional recovery post-transplantation [21]. FLRT3, which was upregulated in d18 cells, is implicated in neurite outgrowth and has been identified as a positive regulator of FGF signaling and cell adhesion [22,23]. FLRT3 codes for a co-receptor for Robo1; the attractive response to the guidance cue Netrin1 has been shown to be controlled by Slit/Robo1 signaling and by FLRT3 [23,24]. Thus, the expression of FLRT3 may promote neurite outgrowth from the grafted d18 precursors. ITGA5 codes for subunit alpha 5 in the integrin alpha chain family (Integrin $\alpha 5\beta 1$), which has been identified as having a role in specific dopaminergic neuron outgrowth onto striatal neurons [25]. Thus, given that the expression of *REST*-regulated genes may be key to identifying the optimal state for transplantation, and several key genes associated with neurite outgrowth are differentially expressed between d18 and d25, there is clear impetus to better understand the role

these genes play as both biomarkers of optimal transplantation and as pathways for modulation to optimize graft efficacy.

It is important to note that, despite working with autologous cell therapy products, using cells harvested from people with PD, the results of the current study are generalisable to all hPSC-derived DA cell therapy products. For example, it is well established that cell maturity can impact upon on graft viability and functionality (e.g. [13,26]). Previous studies have demonstrated that individual cell therapy products are likely to each have an optimal day of harvest for transplantation, making it critical to determine this timepoint for each cell line or batch. In contrast to our study, however, a previous study investigating the effect of differentiation state on graft outcome used one cell line and identified graft size and total TH+ neuron content as the key factor driving graft efficacy [13]. Here, we present evidence, across two cell lines, that similarly sized grafts, with comparable TH neuron content, may not produce equivalent behaviour. Instead, the key determinate is the extent to which grafts integrate into the host brain, not the size of the graft *per se*. Finally, we present corresponding gene expression data to further characterise these distinct cell products and we identify *REST* as a potentially exciting biomarker of optimal cell state.

Our study is unique in that we have distinguished two distinct cell preparations that are both capable of surviving long-term *in vivo* and producing dopamine neuron-rich grafts in a rat model of PD, but observed that only one of the cell profiles restored motor function. The effective cells behaved differently in the host brain, producing extensive neurite outgrowth. It is important to note that different differentiation protocols result in distinct maturation timescales, so the specific number of days in culture that produces optimal *in vivo* transplants will differ according to the protocol[13,26–28]. Our work does suggest, however, that it is likely that the optimal time of differentiation before transplantation may be identifiable for all protocols. Phenotyping cultures by gene expression analysis offers insights into the characteristics that distinguish cells that develop into effective grafts from those that fail, and is useful for discovering markers that can predict the success of cultures. Gene expression profiles may be used to identify an optimized product to ensure extensive neurite outgrowth after grafting and consequent functional recovery.

This is especially important for autologous cell replacement therapy for PD[29] for which effective cell types must be derived reproducibly from each graft recipient.

Acknowledgements

MJL was supported by a Parkinson's UK Senior Research Fellowship (F-1502); RH was supported by a grant from Summit for Stem Cell Foundation; JFL, HT, ABL, and RMW were supported by grants from Summit for Stem Cell Foundation and the California Institute for Regenerative Medicine (CIRM; CL1-00502, RT3-07655, GC1R-06673-A). JFL, HT, ABL, RMW and DGS were supported by CIRM (DISC2-09073); PPS and IVS were supported by NIH (DA046170, DA046204-04, DA043268). The authors wish to acknowledge our Scripps colleague, Loren (Larry) H. Parsons (1964-2016) for the use of his laboratory for HPLC analysis.

An earlier draft of this manuscript was posted as a preprint at bioRxiv (DOI:10.1101/2022.04.19.488213).

Disclosure of Potential Conflicts of Interest

There are no conflicts of interest. All of the data were generated at Scripps Research Institute or Cardiff University with the financial support indicated. JFL and ABL are stockholders and founders of Aspen Neuroscience, Inc. (Aspen). HT, RMW, and JAM are stockholders in Aspen.

References

1. Henchcliffe C and Parmar M. (2018). Repairing the brain: Cell replacement using stem cell-based technologies. *Journal of Parkinson's Disease*. IOS Press; 8(s1), S131–S137. <https://doi.org/10.3233/JPD-181488>
2. Barker RA, Barrett J, Mason SL, Björklund A. (2013). Fetal dopaminergic transplantation trials and the future of neural grafting in Parkinson's disease. *Lancet Neurol*. 12(1):84–91. Available from: <http://www.ncbi.nlm.nih.gov/pubmed/23237903>
3. Li W, Englund E, Widner H, Mattsson B, van Westen D, Lätt J, Rehncrona S, Brundin P, Björklund A, Lindvall O, & Li J Y. (2016). Extensive graft-derived dopaminergic innervation is maintained 24 years after transplantation in the degenerating parkinsonian brain. *Proceedings of the National Academy of Sciences of the United States of America*, 113(23), 6544–6549. <https://doi.org/10.1073/pnas.16052451134>.
4. Grealish S, Heuer A, Cardoso T, Kirkeby A, Jönsson M, Johansson J, & Palmer M. (2015). Monosynaptic Tracing using Modified Rabies Virus Reveals Early and Extensive Circuit Integration of Human Embryonic Stem Cell-Derived Neurons. *Stem Cell Reports*. 4(6):975–83. Available from: <https://linkinghub.elsevier.com/retrieve/pii/S221367111500123X>
5. Kirkeby A, Grealish S, Wolf DA, Nelander J, Wood J, Lundblad M, Lindvall O, & Parmar, M. (2012). Generation of regionally specified neural progenitors and functional neurons from human embryonic stem cells under defined conditions. *Cell reports*, 1(6), 703–714. <https://doi.org/10.1016/j.celrep.2012.04.0096>.
6. Kriks S, Shim JW, Piao J, Ganat YM, Wakeman DR, Xie Z, Carrillo-Reid L, Auyeung G, Antonacci C, Buch A, Yang L, Beal MF, Surmeier DJ, Kordower JH, Tabar V, Studer L. (2011). Dopamine neurons derived from human ES cells efficiently engraft in animal models of Parkinson's disease. *Nature*. 480(7378):547-51. doi: 10.1038/nature10648. PMID: 22056989; PMCID: PMC3245796.

7. Lelos MJ, Morgan RJ, Kelly CM, Torres EM, Rosser AE, Dunnett SB. (2016). Amelioration of non-motor dysfunctions after transplantation of human dopamine neurons in a model of Parkinson's disease. *Exp Neurol*. 278:54-61. doi: 10.1016/j.expneurol.2016.02.003.
8. Barker RA, Parmar M, Studer L, Takahashi J. (2017). Human Trials of Stem Cell-Derived Dopamine Neurons for Parkinson's Disease: Dawn of a New Era. *Cell Stem Cell*. 21(5):569–73. Available from: <http://www.ncbi.nlm.nih.gov/pubmed/29100010>
9. Schweitzer JS, Song B, Herrington TM, Park TY, Lee N, Ko S, Jeon J, Cha Y, Kim K, Li Q, Henchcliffe C, Kaplitt M, Neff C, Rapalino O, Seo H, Lee IH, Kim J, Kim T, Petsko GA, Ritz J, Cohen BM, Kong SW, Leblanc P, Carter BS, Kim KS. (2010). Personalized iPSC-Derived Dopamine Progenitor Cells for Parkinson's Disease. *N Engl J Med*. 14;382(20):1926-1932. doi: 10.1056/NEJMoa1915872. PMID: 32402162; PMCID: PMC7288982.
10. Kim TW, Koo SY, Studer L. (2020). Pluripotent Stem Cell Therapies for Parkinson Disease: Present Challenges and Future Opportunities. *Front Cell Dev Biol*. 8:729. Available from: <https://pubmed.ncbi.nlm.nih.gov/32903681/>
11. Takahashi J. (2020). iPS cell-based therapy for Parkinson's disease: A Kyoto trial. *Regen Ther*. 13:18–22. Available from: <https://pubmed.ncbi.nlm.nih.gov/33490319/>
12. Love MI, Huber W, Anders S. (2014). Moderated estimation of fold change and dispersion for RNA-seq data with DESeq2. *Genome Biol [Internet]*. 15:550. Available from: <https://pubmed.ncbi.nlm.nih.gov/25516281/>
13. Hiller BM, Marmion DJ, Thompson CA, Elliott NA, Federoff H, Brundin P, Mattis VB, McMahon CW, Kordower JH. (2022). Optimizing maturity and dose of iPSC-derived dopamine progenitor cell therapy for Parkinson's disease. *NPJ Regen Med*. 7(1):24. doi: 10.1038/s41536-022-00221-y. PMID: 35449132; PMCID: PMC9023503.
14. Kirkeby A, Nolbrant S, Tiklova K, Heuer A, Kee N, Cardoso T, Ottosson DR, Lelos MJ, Rifés P, Dunnett SB, Grealish S, Perlmann T, Parmar M. (2017). Predictive Markers

Guide Differentiation to Improve Graft Outcome in Clinical Translation of hESC-Based Therapy for Parkinson's Disease. *Cell Stem Cell*. 20(1):135-148. doi: 10.1016/j.stem.2016.09.004. Epub 2016 Oct 27. PMID: 28094017; PMCID: PMC5222722.

15. International Stem Cell Initiative. Assessment of established techniques to determine developmental and malignant potential of human pluripotent stem cells. (2018). *Nat Commun*. 9(1):1925. doi: 10.1038/s41467-018-04011-3. PMID: 29765017; PMCID: PMC5954055.
16. Müller FJ, Laurent LC, Kostka D, Ulitsky I, Williams R, Lu C, Park IH, Rao MS, Shamir R, Schwartz PH, Schmidt NO, Loring JF. (2008). Regulatory networks define phenotypic classes of human stem cell lines. *Nature*. 455(7211):401-5. doi: 10.1038/nature07213. Epub 2008 Aug 24. PMID: 18724358; PMCID: PMC2637443.
17. Bhuiyan MIH, Lee JH, Kim SY, Cho KO. (2013). Expression of exogenous LIN28 contributes to proliferation and survival of mouse primary cortical neurons in vitro. *Neuroscience*. 248:448–58. Available from: <https://pubmed.ncbi.nlm.nih.gov/23806711/>
18. Wang XW, Li Q, Liu CM, Hall PA, Jiang JJ, Katchis CD, Kang S, Dong BC, Li S, Zhou FQ. (2018). Lin28 Signaling Supports Mammalian PNS and CNS Axon Regeneration. *Cell Rep*. 24(10):2540-2552.e6. doi: 10.1016/j.celrep.2018.07.105. PMID: 30184489; PMCID: PMC6173831.
19. Xia X, Teotia P, Ahmad I. (2018). Lin28a regulates neurogliogenesis in mammalian retina through the Igf signaling. *Dev Biol* 440(2):113–28. Available from: <https://pubmed.ncbi.nlm.nih.gov/29758178/>
20. Nathan FM, Ohtake Y, Wang S, Jiang X, Sami A, Guo H, Zhou FQ, Li S. (2020). Upregulating Lin28a Promotes Axon Regeneration in Adult Mice with Optic Nerve and Spinal Cord Injury. *Mol Ther*. 28(8):1902-1917. doi: 10.1016/j.ymthe.2020.04.010. Epub 2020 Apr 15. PMID: 32353321; PMCID: PMC7403348.

21. Rhee YH, Kim TH, Jo AY, Chang MY, Park CH, Kim SM, Song JJ, Oh SM, Yi SH, Kim HH, You BH, Nam JW, Lee SH. (2016). LIN28A enhances the therapeutic potential of cultured neural stem cells in a Parkinson's disease model. *Brain*. 139(Pt 10):2722-2739. doi: 10.1093/brain/aww203. Epub 2016 Aug 18. PMID: 27538419.
22. Robinson M, Parsons Perez MC, Tébar L, Palmer J, Patel A, Marks D, Sheasby A, De Felipe C, Coffin R, Livesey FJ, Hunt SP. (2004). FLRT3 is expressed in sensory neurons after peripheral nerve injury and regulates neurite outgrowth. *Mol Cell Neurosci*. 27(2):202-14. doi: 10.1016/j.mcn.2004.06.008. PMID: 15485775.
23. Tsuji L, Yamashita T, Kubo T, Madura T, Tanaka H, Hosokawa K, Tohyama M. (2004). FLRT3, a cell surface molecule containing LRR repeats and a FNIII domain, promotes neurite outgrowth. *Biochem Biophys Res Commun*. 313(4):1086-91. doi: 10.1016/j.bbrc.2003.12.047. PMID: 14706654.
24. Leyva-Díaz E, del Toro D, Menal MJ, Cambray S, Susín R, Tessier-Lavigne M, Klein R, Egea J, López-Bendito G. (2014). FLRT3 is a Robo1-interacting protein that determines Netrin-1 attraction in developing axons. *Curr Biol*. 24(5):494-508. doi: 10.1016/j.cub.2014.01.042. Epub 2014 Feb 20. PMID: 24560577.
25. Izumi Y, Wakita S, Kanbara C, Nakai T, Akaike A, Kume T. (2017). Integrin $\alpha 5\beta 1$ expression on dopaminergic neurons is involved in dopaminergic neurite outgrowth on striatal neurons. *Sci Rep*. 7, 42111. Available from: <https://pubmed.ncbi.nlm.nih.gov/28176845/>
26. de Luzy IR, Pavan C, Moriarty N, Hunt CPJ, Vandenhoven Z, Khanna A, Niclis JC, Gantner CW, Thompson LH, Parish CL. (2022). Identifying the optimal developmental age of human pluripotent stem cell-derived midbrain dopaminergic progenitors for transplantation in a rodent model of Parkinson's disease. *Exp Neurol*. 358:114219. doi: 10.1016/j.expneurol.2022.114219. Epub 2022 Aug 30. PMID: 36055392.
27. Qiu L, Liao MC, Chen AK, Wei S, Xie S, Reuveny S, Zhou ZD, Hunziker W, Tan EK, Oh SKW, Zeng L. (2017). Immature Midbrain Dopaminergic Neurons Derived from Floor-

Plate Method Improve Cell Transplantation Therapy Efficacy for Parkinson's Disease. *Stem Cells Transl Med.* 6(9):1803-1814. doi: 10.1002/sctm.16-0470. Epub 2017 Jun 26. PMID: 28650520; PMCID: PMC5689771.

28. Song B, Cha Y, Ko S, Jeon J, Lee N, Seo H, Park KJ, Lee IH, Lopes C, Feitosa M, Luna MJ, Jung JH, Kim J, Hwang D, Cohen BM, Teicher MH, Leblanc P, Carter BS, Kordower JH, Bolshakov VY, Kong SW, Schweitzer JS, Kim KS. (2020). Human autologous iPSC-derived dopaminergic progenitors restore motor function in Parkinson's disease models. *J Clin Invest.* 130(2):904-920. doi: 10.1172/JCI130767. PMID: 31714896; PMCID: PMC6994130.
29. Loring JF. (2018). Autologous Induced Pluripotent Stem Cell-Derived Neurons to Treat Parkinson's Disease. *Stem Cells Dev* 27(14):958–9. Available from: <https://pubmed.ncbi.nlm.nih.gov/29790422/>
30. Benjamini Y, Hochberg Y. (1995). Controlling the False Discovery Rate: A Practical and Powerful Approach to Multiple Testing. *Journal of the Royal Statistical Society Series B (Methodological).* 57(1):289–300.
31. Brundin P, Nilsson OG, Gage FH, Björklund A. (1985). Cyclosporin A increases survival of cross-species intrastriatal grafts of embryonic dopamine-containing neurons. *Exp Brain Res* 60(1):204–8. Available from: <https://pubmed.ncbi.nlm.nih.gov/3930278/>
32. Rath A, Klein A, Papazoglou A, Pruszek J, Garcia J, Krause M, Maciaczyk J, Dunnett SB, Nikkhah G. (2013). Survival and functional restoration of human fetal ventral mesencephalon following transplantation in a rat model of Parkinson's disease. *Cell Transplant.* 22(7):1281-93. doi: 10.3727/096368912X654984. Epub 2012 Sep 7. PMID: 22963760.
33. Grealish S, Diguët E, Kirkeby A, Mattsson B, Heuer A, Bramouille Y, Van Camp N, Perrier AL, Hantraye P, Björklund A, Parmar M. (2014). Human ESC-derived dopamine neurons show similar preclinical efficacy and potency to fetal neurons when grafted in a rat model of Parkinson's disease. *Cell Stem Cell.* 15(5):653-65. doi:

10.1016/j.stem.2014.09.017. Epub 2014 Nov 6. PMID: 25517469; PMCID: PMC4232736.

34. Glenn VL, Schell JP, Fakunle ES, Simon R, Peterson SE. (2012). Isolation of Human Dermal Fibroblasts from Biopsies. In: Loring JF, Peterson SE, editors. *Human Stem Cell Manual*. London: Elsevier Inc. p. 129–41.
35. Boland MJ, Nazor KL, Tran HT, Szücs A, Lynch CL, Paredes R, Tassone F, Sanna PP, Hagerman RJ, Loring JF. (2017). Molecular analyses of neurogenic defects in a human pluripotent stem cell model of fragile X syndrome. *Brain*. 140(3):582-598. doi: 10.1093/brain/aww357. PMID: 28137726; PMCID: PMC5837342.
36. Kilpinen H, Goncalves A, Leha A, Afzal V, Alasoo K, Ashford S, Bala S, Bensaddek D, Casale FP, Culley OJ, Danecek P, Faulconbridge A, Harrison PW, Kathuria A, McCarthy D, McCarthy SA, Meleckyte R, Memari Y, Moens N, Soares F, Mann A, Streeter I, Agu CA, Alderton A, Nelson R, Harper S, Patel M, White A, Patel SR, Clarke L, Halai R, Kirton CM, Kolb-Kokocinski A, Beales P, Birney E, Danovi D, Lamond AI, Ouwehand WH, Vallier L, Watt FM, Durbin R, Stegle O, Gaffney DJ. (2017). Common genetic variation drives molecular heterogeneity in human iPSCs. *Nature*. 546(7658):370-375. doi: 10.1038/nature22403. Epub 2017 May 10. Erratum in: *Nature*. 2017 Jun 29;546(7660):686. PMID: 28489815; PMCID: PMC5524171.
37. Ewels PA, Peltzer A, Fillinger S, Patel H, Alneberg J, Wilm A, Garcia MU, Di Tommaso P, Nahnsen S. (2020). The nf-core framework for community-curated bioinformatics pipelines. *Nat Biotechnol*. 38(3):276-278. doi: 10.1038/s41587-020-0439-x. PMID: 32055031.
38. Patro R, Duggal G, Love MI, Irizarry RA, Kingsford C. (2017). Salmon provides fast and bias-aware quantification of transcript expression. *Nat Methods* 14(4):417–9. Available from: <https://pubmed.ncbi.nlm.nih.gov/28263959/>
39. Robinson MD, McCarthy DJ, Smyth GK. (2010). edgeR: a Bioconductor package for differential expression analysis of digital gene expression data. *Bioinformatics* 26(1):139–40. Available from: <https://pubmed.ncbi.nlm.nih.gov/19910308/>

40. Benjamini Y, Hochberg Y. (1995). Controlling The False Discovery Rate - A Practical And Powerful Approach To Multiple Testing. *Journal of the Royal Statistical Society Series B: Methodological*. 57:289–300.
41. Clarke DJB, Kuleshov MV, Schilder BM, Torre D, Duffy ME, Keenan AB, Lachmann A, Feldmann AS, Gundersen GW, Silverstein MC, Wang Z, Ma'ayan A. (2018). eXpression2Kinases (X2K) Web: linking expression signatures to upstream cell signaling networks. *Nucleic Acids Res*. 46(W1):W171-W179. doi: 10.1093/nar/gky458. PMID: 29800326; PMCID: PMC6030863.
42. Lachmann A, Ma'ayan A. KEA: (2009). Kinase enrichment analysis. *Bioinformatics*.25(5):684–6. Available from: <https://pubmed.ncbi.nlm.nih.gov/19176546/>
43. Chen EY, Xu H, Gordonov S, Lim MP, Perkins MH, Ma'ayan A. (2012). Expression2Kinases: mRNA profiling linked to multiple upstream regulatory layers. *Bioinformatics* 28(1):105–11. Available from: <https://pubmed.ncbi.nlm.nih.gov/22080467/>
44. Eden E, Navon R, Steinfeld I, Lipson D, Yakhini Z. (2009). GOrilla: A tool for discovery and visualization of enriched GO terms in ranked gene lists. *BMC Bioinformatics* 10. Available from: <https://pubmed.ncbi.nlm.nih.gov/19192299/>
45. Timmons JA, Szkop KJ, Gallagher IJ. (2015). Multiple sources of bias confound functional enrichment analysis of global -omics data. *Genome Biol* 16(1). Available from: <https://pubmed.ncbi.nlm.nih.gov/26346307/>
46. Tiklová K, Nolbrant S, Fiorenzano A, Björklund ÅK, Sharma Y, Heuer A, Gillberg L, Hoban DB, Cardoso T, Adler AF, Birtele M, Lundén-Miguel H, Volakakis N, Kirkeby A, Perlmann T, Parmar M. (2020). Single cell transcriptomics identifies stem cell-derived graft composition in a model of Parkinson's disease. *Nat Commun*. 2020 May 15;11(1):2434. doi: 10.1038/s41467-020-16225-5. Erratum in: *Nat Commun*. 2020 Jul 15;11(1):3630. PMID: 32415072; PMCID: PMC7229159.

47. Björklund A, Dunnett SB. (2019). The Amphetamine Induced Rotation Test: A Re-Assessment of Its Use as a Tool to Monitor Motor Impairment and Functional Recovery in Rodent Models of Parkinson's Disease. *J Parkinsons Dis.* 9(1):17-29. doi: 10.3233/JPD-181525. PMID: 30741691; PMCID: PMC6398560.
48. Dunnett SB, Brooks SP. (2018). Motor Assessment in Huntington's Disease Mice. *Methods Mol Biol.* 1780:121–41. Available from: <https://pubmed.ncbi.nlm.nih.gov/29856017/>
49. Bagga V, Dunnett SB, Fricker-Gates RA. (2008). Ascorbic acid increases the number of dopamine neurons in vitro and in transplants to the 6-OHDA-lesioned rat brain. *Cell Transplant.* 17(7):763–73. Available from: <https://pubmed.ncbi.nlm.nih.gov/19044203/>

Figure Legends

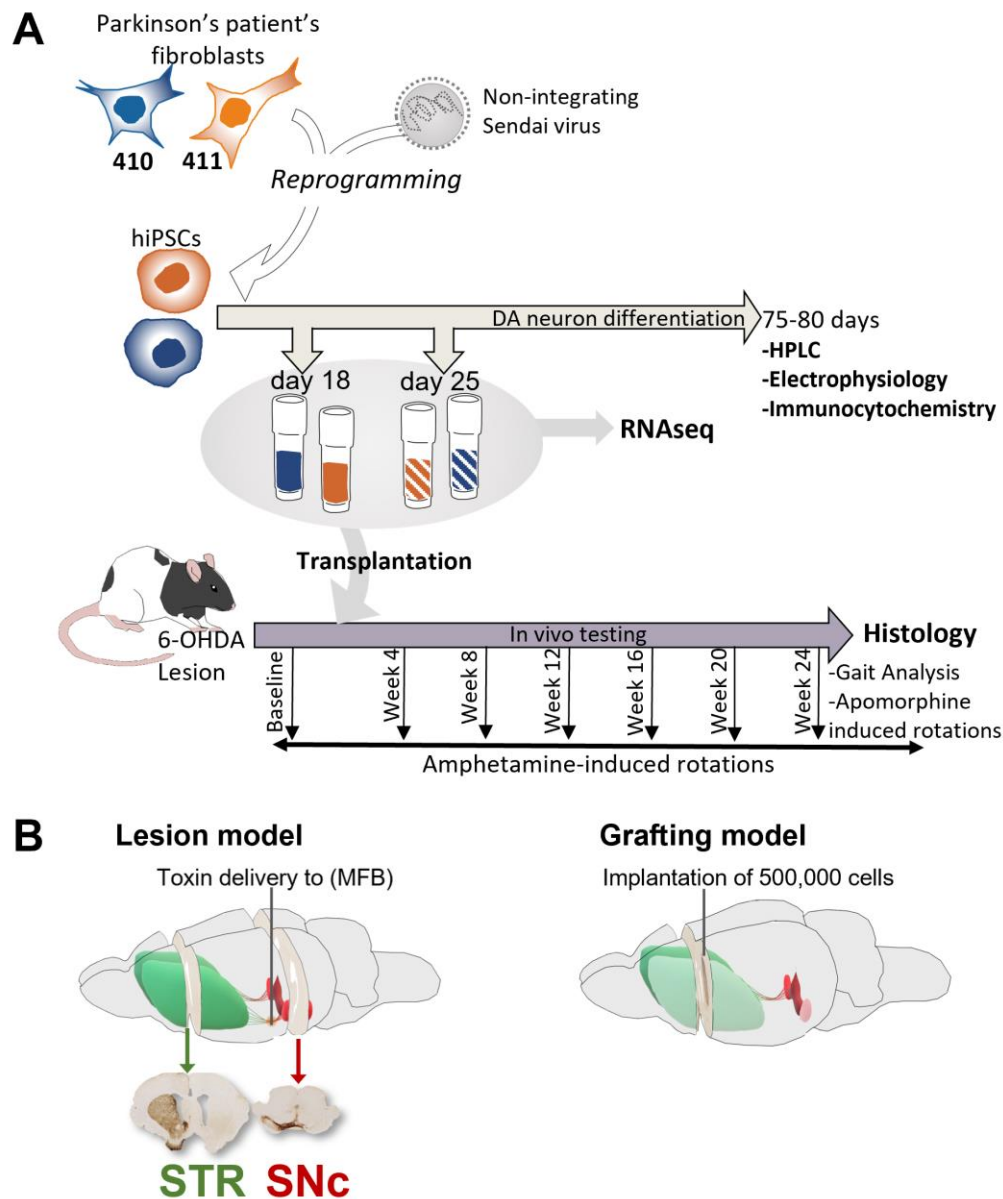


Figure 1. Experimental Overview. (A) Study design showing experimental progression from fibroblasts to transplant-stage neuronal precursors, and the main outcome measures from both *in vitro* and *in vivo* investigation of their suitability as a dopamine neuron replacement source. (B) Schematics showing unilateral 6-OHDA medial forebrain bundle (MFB) lesion model with accompanying unilateral TH depletion in immunolabelled brain sections in the striatum (STR) and substantia nigra pars compacta (SNc) (left), and cell replacement strategy, which consists of surgical implantation of cells into the striatum (right).

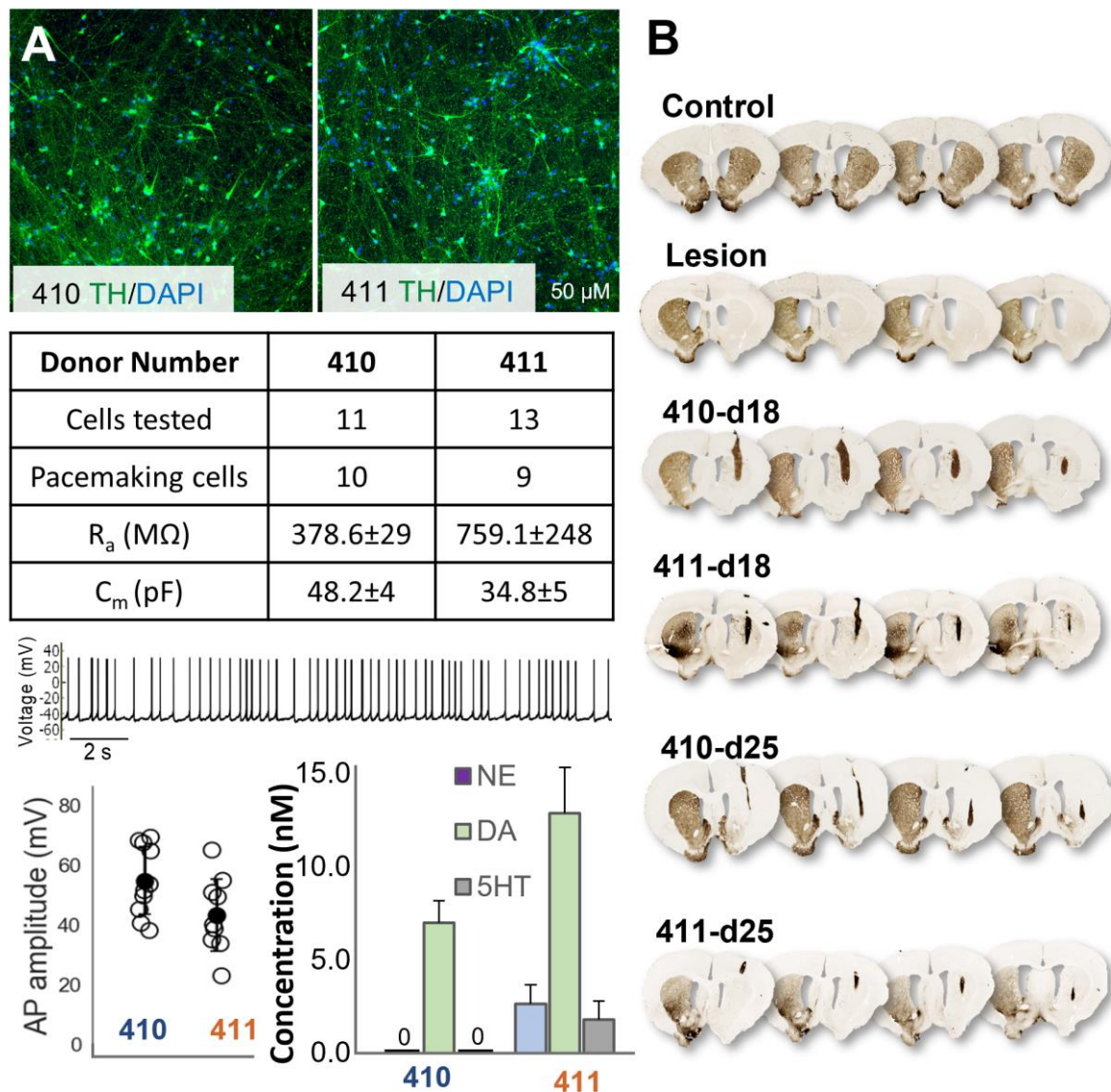


Figure 2: Characterization of dopaminergic neuron differentiation and maturation from two PD donor iPSC lines. (A) iPSCs from 410 and 411 cell lines that were differentiated to day 80 *in vitro* express dopamine neuron marker tyrosine hydroxylase (TH; green). Single-cell patch clamp analysis of day 75 cells showed that most of the neurons had pace making activity and mature membrane resistance (R_a) and capacitance (C_m). Action potential amplitudes were maintained close to 60mV. HPLC analysis of day 88-89 cultures stimulated with KCl shows release of dopamine (DA) and small amounts of norepinephrine (NE) and serotonin (5-HT). (B) Representative examples of immunohistochemical analysis of TH+ grafts in Control, Lesion, d18 and d25 graft groups.

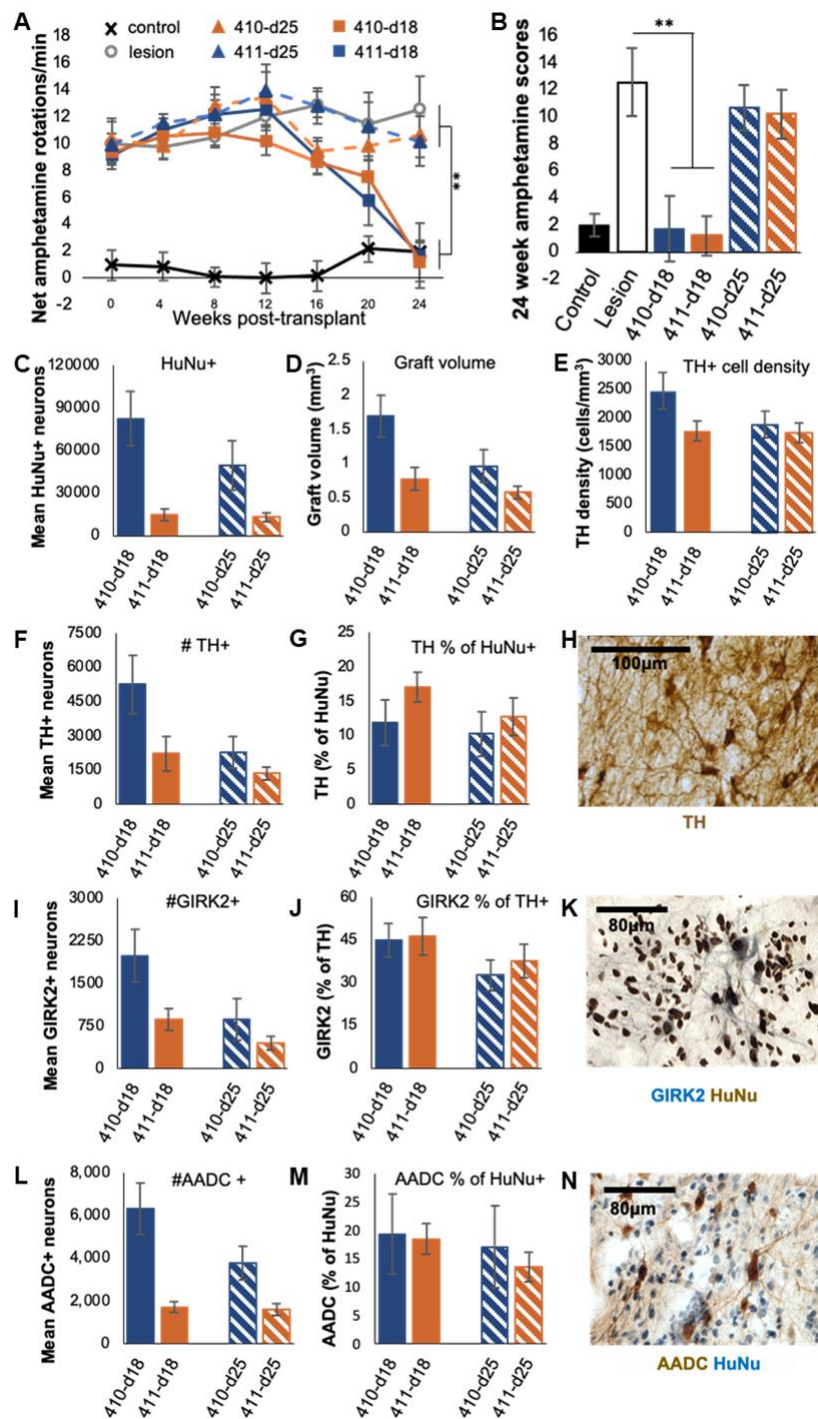


Figure 3. Effect of iPSC-derived cells on motor function and immunohistochemical analysis of d18 and d25 iPSC-derived grafts. (A) Raw data showing performance of Control, Lesion, 410-d18, 411-d18, 410-d25 and 411-25 grafted rats on amphetamine-induced rotation test across the full test period, and (B) net rotation score at 24 weeks post-graft only. Based on histological analysis of the grafts from d18 and d25 preparations, we present (C) the total mean HuNu+ cells, (D) graft volume, (E) the density of TH+ cells per

*mm³, (F) total TH+ neurons, (G) percentage of TH+ cells out of total HuNu+ cells, (I) the total GIRK2+ cells and (J) the percentage of GIRK2+ cells out of TH+ cells. The total AADC+ cell data are depicted in (L) and the percentage of AADC+ cells relative to HuNu+ cells is in (M). Representative immunohistochemistry is presented for (H) TH, (K) GIRK2 (blue) and HuNu (brown) and (N) AADC (brown) and HuNu (blue). p**≤0.001, error bars= ±SEM.*

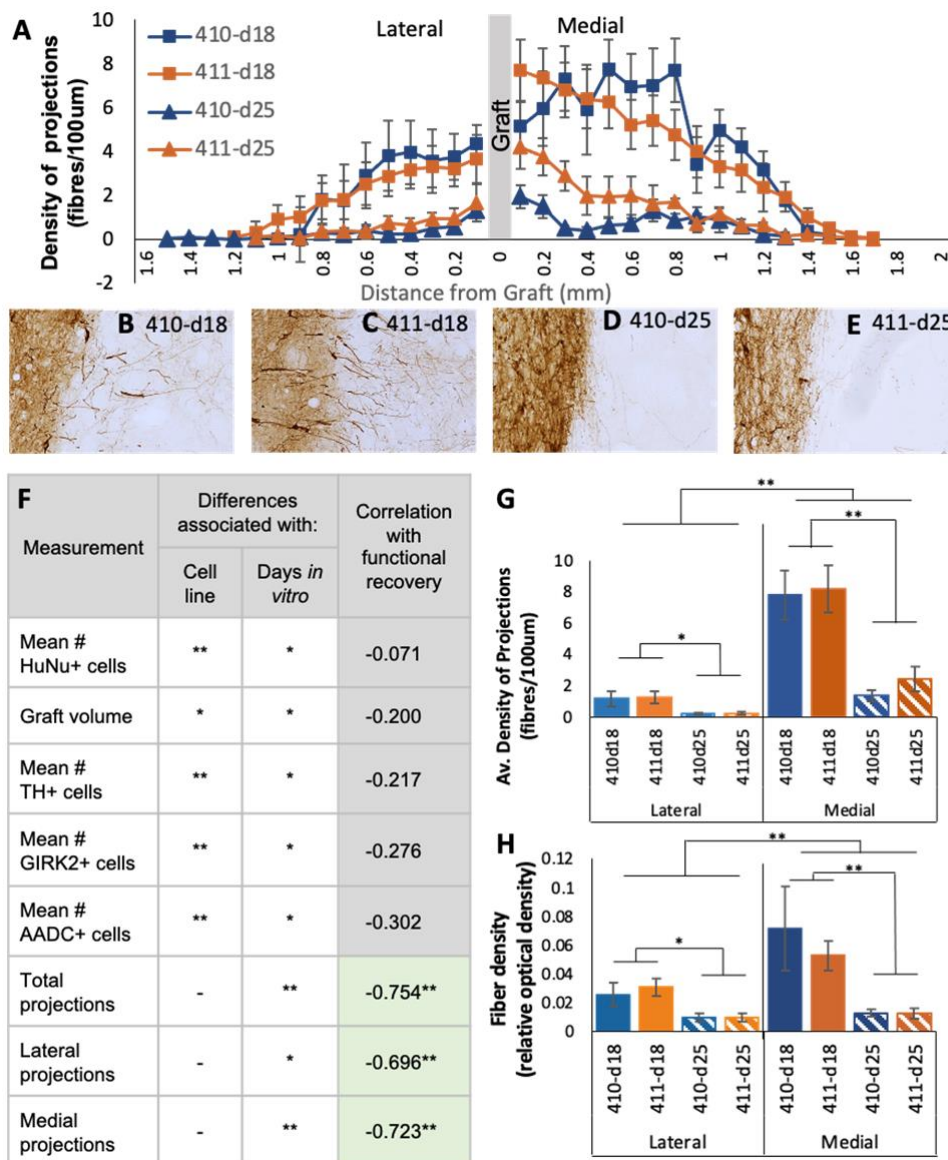


Figure 4. Greater innervation from d18 grafts. (A) Differences were evident in neurite outgrowth from the d18 and 25 grafts into the surrounding host striatum up to 1400µm from the graft border. (B-E) Representative images of TH+ neurites. (F) Functional recovery did not correlate with graft volume or cellular composition of the grafts. Functional recovery did correlate significantly with greater overall neurite outgrowth and greater fiber projections into both lateral and medial neostriatum (* $p \leq 0.01$; ** $p \leq 0.001$). (G) Manual counting of fibers revealed 4-fold higher average density of projections from d18 grafts compared to d25 grafts. (H) Significantly more neurite outgrowth was also evident in d18 grafts when the tissue was analyzed using unbiased optical density estimates via computerized image analysis (Image-J). Analysis of the y-intercept of projection trend lines

confirmed significantly more neurite outgrowth from d18 grafts (Supplemental Figure 1C). This is further supported by correlation analysis of both projection density measurements and optical density of projection fibers (Supplemental Figure 1E-J).

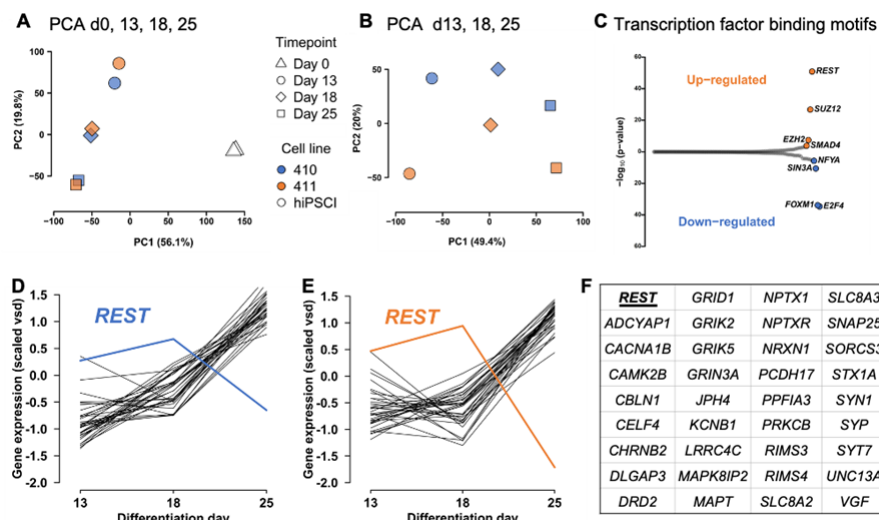


Figure 5. Gene expression analysis. RNA was sequenced at the two stages used for efficacy assessment (d18 and d25) and two earlier stages, day 0 (undifferentiated iPSCs) and d13 of differentiation. **A.** Principal component one (PC1) explained 56.1% of the variance in transcriptome expression in the d0, d13, d18, and d25 data set and largely separated the undifferentiated cells (triangles: day 0) from the differentiating dopaminergic precursors (circles, diamonds and squares representing day 13, day 18 and day 25, respectively). The second axis (PC2) delineated the DA precursors in a rank order corresponding with their development duration. **B.** Comparison of the differentiation stages (d13, d18, d25) showed a strong signal of development stage along PC1 (49.4% of transcriptome variance) and PC2 separated the two cell lines (410: blue and 411: orange) within a time point. **C.** Transcription factor binding site motifs in differentially expressed genes that were enriched in genes upregulated and downregulated between d18 and d25 of differentiation. Genes regulated by the repressors REST (RE1 Silencing Transcription Factor) and SUZ12 (SUZ12 Polycomb Repressive Complex 2 Subunit) were expressed at higher levels at d25. Day 25 cells had lower levels of genes regulated by cell cycle-associated factors FOXM1 (Forkhead Box M1) and EFF4 (E2F transcription factor 4). **D.** and **E.** Normalized, zero-centered gene expression levels of REST and neuronal genes repressed by REST. As cells differentiated, REST decreased and REST targets increased in both iPSC line 410 (D) and iPSC line 411 (E). **F.** List of neuron-associated genes with REST motifs upregulated at d25.

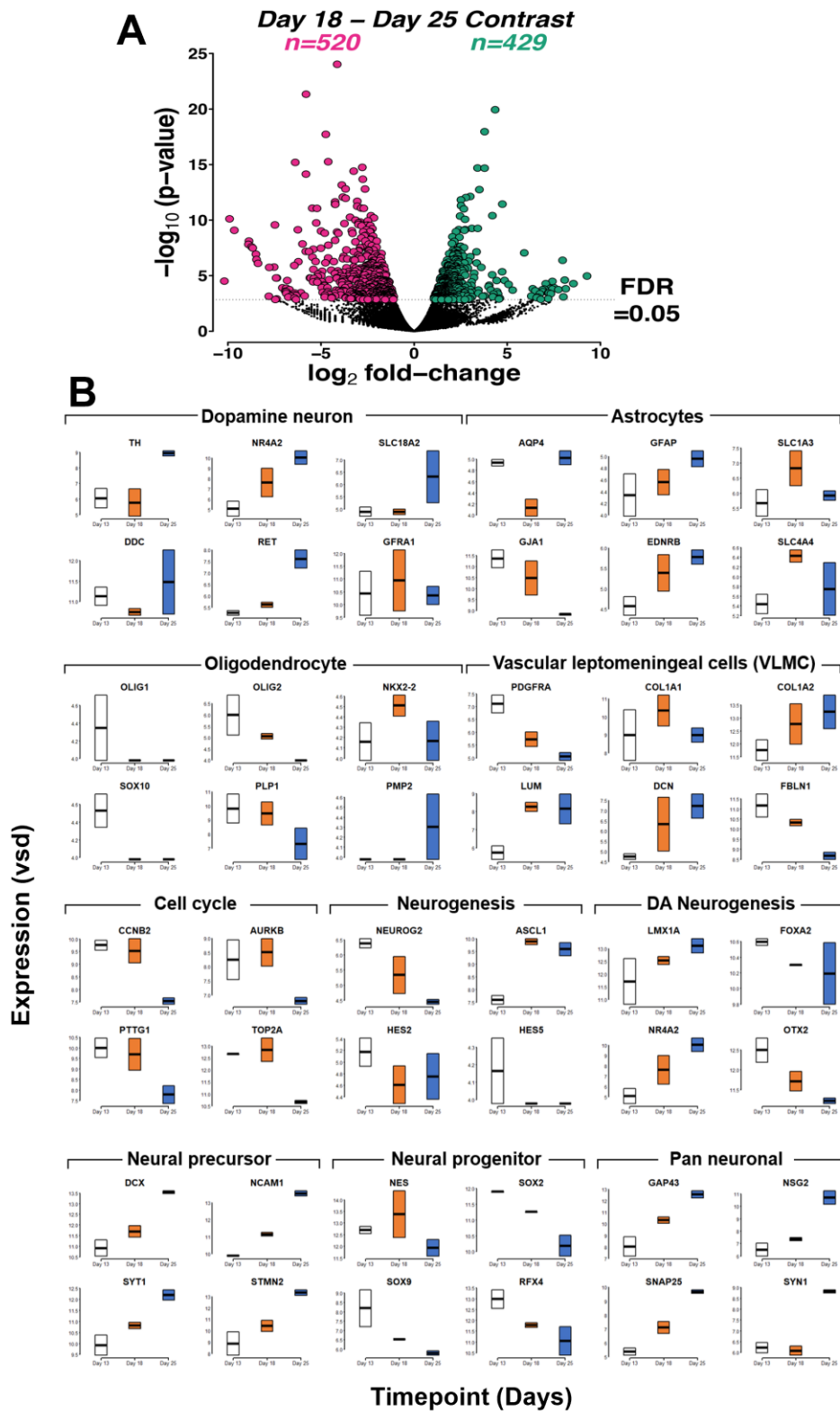


Figure 6: RNAseq analysis of cell preparations. (A) A volcano plot showing that a total of 520 genes were up-regulated at day 25 relative to day 18 (pink). 429 genes were down-regulated between day 18 and day 25 (green) (FDR<0.05). (B) RNAseq data for cell

preparations harvested at d13, d18 and d25, with genes grouped according to association with cell type or stage. Expression values are displayed as variance stabilized data (vsd), calculated using the vst command in the DESeq2 package[12].